Search for the Standard Model Higgs boson in $WH \to l\nu bb$ and $H \to WW^{(*)} \to l\nu l\nu$ channels at ATLAS

Lashkar Kashif on behalf of ATLAS
Department of Physics, University of Wisconsin, Madison, WI, USA

Results for the Standard Model Higgs boson search by the ATLAS experiment in the $WH \to l\nu bb$ and $H \to WW^{(*)} \to l\nu l\nu$ channels are presented. The results are based on 1.04 fb^{-1} of data from $p\bar{p}$ collisions at $\sqrt{s} = 7$ TeV produced by the LHC in 2011. No evidence is found for the Standard Model Higgs boson in either decay mode. The $WH \to l\nu bb$ channel is not yet sensitive to the Standard Model Higgs, while the $H \to WW^{(*)} \to l\nu l\nu$ channel excludes the Standard Model Higgs in the range of $158 < m_{\rm H} < 186$ GeV at the 95% confidence level.

arXiv:1109.4747v2 [hep-ex] 27 Sep 2011

1. Introduction

$WH \to l\nu bb$ and $H \to WW^{(*)} \to l\nu l\nu$ are two of the most important channels to search for the Standard Model (SM) Higgs boson, together covering the theoretically allowed Higgs mass range. In this talk, we present Higgs search results in these channels by the ATLAS experiment at the CERN Large Hadron Collider (LHC).

The data sample used in these analyses was collected by ATLAS during the period March-June 2011, and corresponds to 1.04 fb^{-1} of integrated luminosity. Figure 1 shows the 7 TeV collision data accumulated by ATLAS in 2011 as function of time. At the time this article is written, the total recorded data correspond to 3.51 fb^{-1}, of which less than one-third was used for the results reported herein. The uncertainty on the luminosity measurement is 3.7%.

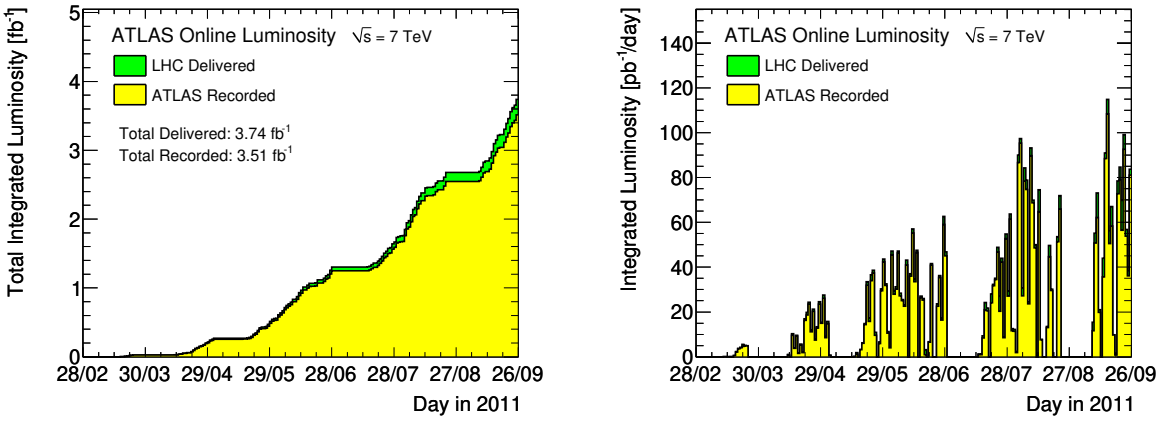


Figure 1: The integrated luminosity collected by the ATLAS experiment between March and August 2011 *(left)*, and the instantaneous luminosity evolution during the same period*(right)*.

Figure 1 also shows the evolution of the instantaneous luminosity $L_{\rm inst}$ as a function of time in 2011. For the results that follow, the maximum $L_{\rm inst}$ reached was 1.26×10^{33} cm^{-2} s^{-1}. The average number of proton-proton interactions per bunch crossing was about 6.

2. The $WH \to l\nu bb$ channel

The $WH \to l\nu bb$ channel takes advantage of the large branching ratio of the $H \to bb$ decay, which is about 2/3 at the Higgs mass $M_{\rm H}$ of 120 GeV (Figure 2). Owing to the very large background of prompt $b\bar{b}$ pairs, a direct search for the $H \to bb$ decay is extremely difficult at the LHC. However, Higgs production associated with a leptonically decaying W or Z boson makes the search easier, since the lepton can be triggered on, and the lepton requirement can be used to reduce the large $b\bar{b}$ background. As a reference, the cross-section $\times$ branching ratio of the process $WH \to l\nu bb$ is about 91 fb for $M_{\rm H} = 120$ GeV.

A cut-based analysis is performed and its strategy is simple: we require two b-tagged jets in addition to W boson search criteria. A Higgs signal would show up as an excess in a $b\bar{b}$ invariant mass spectrum.

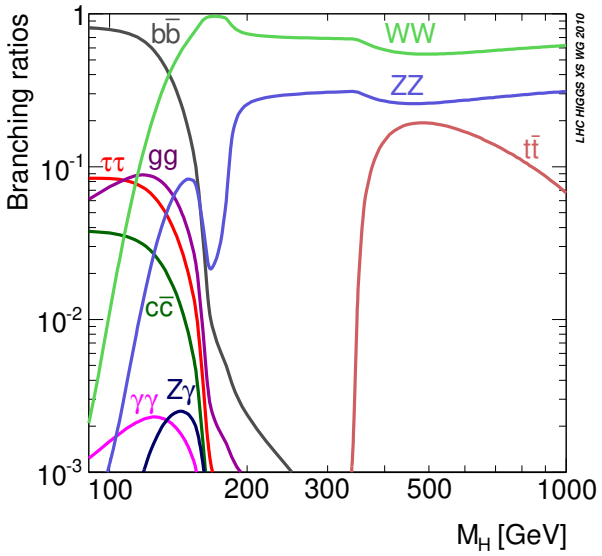


Figure 2: The branching ratio of the Standard Model Higgs boson into various final states as a function of the Higgs mass.

2.1. Event selection

Since the W boson can decay into an electron or a muon, the analysis is performed separately for the electron and muon channels. In each channel, we require that events pass the lowest-threshold unprescaled trigger: this threshold is 20 GeV and 18 GeV for the electron and muon channels respectively. Further event selection criteria are listed below:

- Exactly one reconstructed lepton in the event. The lepton must have at least 25 GeV transverse momentum (p_{T}). An electron must be within the pseudorapidity range $|\eta| < 2.47$; a muon must be within $|\eta| < 2.4$.
- Exactly two jets in the event, reconstructed using the anti-k_{T} algorithm with a distance parameter R = 0.4. Each jet must have $p_{\mathrm{T}} > 25$ GeV and be within $|\eta| < 2.5$. In addition, each jet must be tagged as a b-jet. Figure 3 *(left)* shows the number of b-tagged jets per event.
- The missing transverse energy, $E_{\mathrm{T}}^{\mathrm{miss}}$, in the event must be larger than 25 GeV.
- The W transverse mass m_{T} must be larger than 40 GeV, where m_{T} is defined as $m_{\mathrm{T}} = \sqrt{2p_{\mathrm{T}}^{\mathrm{l}}p_{\mathrm{T}}^{\nu}(1-\cos(\phi^{\mathrm{l}}-\phi^{\nu}))}$. $p_{\mathrm{T}}^{\mathrm{l}}$ is the lepton p_{T}, $p_{\mathrm{T}}^{\nu} = E_{\mathrm{T}}^{\mathrm{miss}}$, and ϕ is the azimuthal angle. Figure 3 *(right)* shows the transverse mass distribution in the electron channel.

2.2. Background processes

Top: $t\bar{t}$ and single top production constitute the largest background to the $WH \to l\nu bb$ channel. These backgrounds are largely reduced by the requirement of exactly two jets in the event. The shape of the residual top background is estimated from Monte Carlo (MC), but the normalization is extracted from a sideband fit in the di-$b$jet invariant mass $m_{\mathrm{b\bar{b}}}$ distribution in data. The sidebands are defined as $m_{\mathrm{b\bar{b}}} < 80$ GeV and $140 < m_{\mathrm{b\bar{b}}} < 250$ GeV.

The shape and normalization of the top background are cross-checked by defining a top control region in data defined by having three jets in the event, two of which must be b-tagged. Figure 4 shows the $m_{\mathrm{b\bar{b}}}$ distribution in this region in data, in top MC and in other backgrounds. We see that the MC gives a reasonable description of both the shape and the normalization seen in data.

W+jets: $W + b\bar{b}$ events constitute a large background at a low $m_{\mathrm{b\bar{b}}}$. The shape of the $W + b\bar{b}$ background is modeled using the shape of the untagged di-jet invariant mass m_{jj} distribution. This modeling is justified

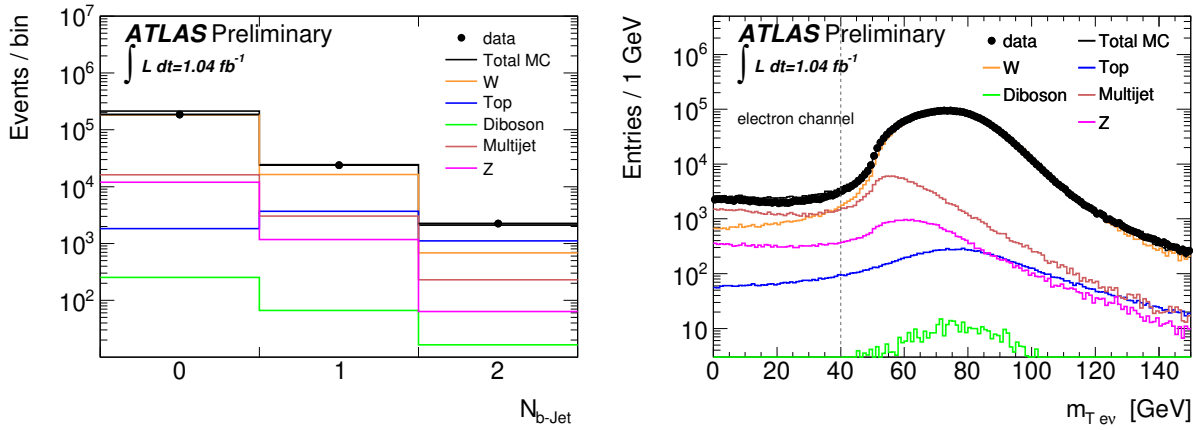


Figure 3: *Left*: Distribution of the number of b-tagged jets per event after the requirement of exactly two jets in the event; *right*: transverse mass spectrum in the electron channel after the cut on $E_{\mathrm{T}}^{\mathrm{miss}}$.

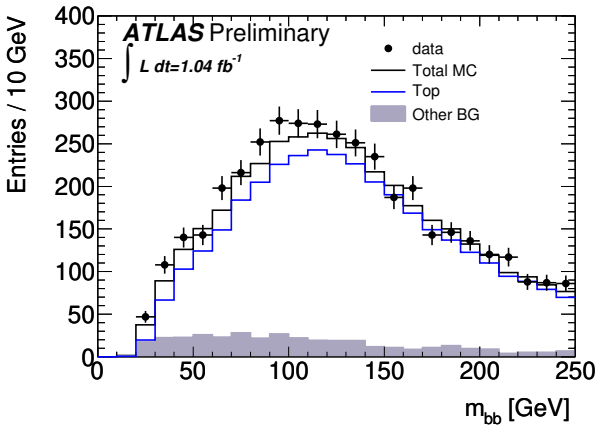


Figure 4: Di-$b$jet invariant mass $m_{\mathrm{b\bar{b}}}$ spectrum in the top control region in data, in top Monte Carlo and in other Monte Carlo-derived backgrounds.

by checking that the shape of the m_{jj} spectrum in untagged *W+jets* events is consistent with that of the $m_{\mathrm{b\bar{b}}}$ spectrum in MC. The template is normalized using a fit to $m_{\mathrm{b\bar{b}}}$ sidebands as for the top background.

QCD: In both electron and muon channels, the QCD background is estimated from data using template fits. QCD-enriched templates in data are obtained by requiring non-isolated leptons; the normalization is derived from fits to the $E_{\mathrm{T}}^{\mathrm{miss}}$ distribution. The process is cross-checked in a QCD control region in data obtained by reversing the $E_{\mathrm{T}}^{\mathrm{miss}}$ and m_{T} cuts.

Diboson: Diboson backgrounds are expected to be very small, and are estimated from MC.

2.3. Systematic uncertainties

Table I summarizes the systematic uncertainties from experimental sources as well as those in the Higgs cross-sections for $m_{\mathrm{H}} = 115$ GeV and $m_{\mathrm{H}} = 130$ GeV. We see that by far the largest source of systematic uncertainty is b-tagging.

2.4. Results

Table II lists the background events expected in 1.04 fb^{-1} of data, the number of data events actually observed and expected signal event count for five different Higgs masses in the range $110 < m_{\mathrm{H}} < 130$ GeV. The numbers were obtained in the range of $40 < m_{\mathrm{b\bar{b}}} < 250$ GeV. We see that the number of observed events is consistent with the predicted background. Figure 5 shows the $m_{\mathrm{b\bar{b}}}$ distribution observed in data as well as the expected

Source of Uncertainty	Effect on $WH \to l\nu bb$ signal	
	$m_{\rm H} = 115$ GeV	$m_{\rm H} = 130$ GeV
Electron Energy Scale	1%	1%
Electron Energy Resolution	1%	1%
Electron Efficiency	1%	1%
Muon Momentum Resolution	4%	1%
Muon Efficiency	1%	1%
Jet Energy Scale	1%	3%
Jet Energy Resolution	1%	1%
Missing Transverse Energy	2%	3%
b-tagging Efficiency	16%	17%
b-tagging Mis-tag Fraction	3%	3%
Luminosity	4%	4%
Higgs Cross-section	5%	5%

Table I: Effect of systematic uncertainties on signal yield for two different Higgs masses.

distribution from MC, the signal prediction having been amplified by a factor of 20 for visibility. We do not see any excess in the observed distribution. We therefore conclude that we do not find any evidence of the SM Higgs in this channel with 1.04 fb^{-1} of data.

Source	expected events	(stat.)	(sys.)
Z+jets	54.4	$\pm$ 3.9	$\pm$ 12.3
W+jets	466.7	$\pm$ 1.4	$\pm$ 66.5
Top-quark	1141.8	$\pm$ 8.8	$\pm$ 78.0
Multijet	193.0	$\pm$ 9.4	$\pm$ 96.5
WZ	16.1	$\pm$ 2.2	$\pm$ 3.4
WW	4.8	$\pm$ 1.1	$\pm$ 1.4
Total background	1876.8	$\pm$ 13.7	$\pm$ 147.2
Data	1888		
Signal $m_{\rm H} = 110$ GeV	6.72	$\pm$ 0.31	$\pm$ 1.20
Signal $m_{\rm H} = 115$ GeV	5.25	$\pm$ 0.30	$\pm$ 0.97
Signal $m_{\rm H} = 120$ GeV	4.54	$\pm$ 0.25	$\pm$ 0.83
Signal $m_{\rm H} = 125$ GeV	4.08	$\pm$ 0.21	$\pm$ 0.77
Signal $m_{\rm H} = 130$ GeV	3.28	$\pm$ 0.17	$\pm$ 0.62

Table II: Expected background events, observed events in data, and predicted signal event count in the range of 40 $< m_{\rm b\bar{b}} <$ 250 GeV. Electron and muon channels are combined. Statistical and systematic uncertainties on the expected background and signal events are shown.

Figure 6 *(left)* shows the exclusion limit on the standardized cross-section $\mu = \sigma/\sigma_{\rm SM}$ at the 95% confidence level. The observed limits are seen to range between 15 to 30 times the SM Higgs cross-section over the Higgs mass range investigated. Figure 6 *(right)* shows the exclusion limit obtained by combining the $ZH \to llbb$ channel with the $WH \to l\nu bb$ channel [1]. The observed limits from the combined search range between 10 to 20 times the SM Higgs cross-section.

3. The $H \to WW^{(*)} \to l\nu l\nu$ channel

$H \to WW^{(*)} \to l\nu l\nu$ ($l = e$ or μ) is a highly sensitive channel in the SM Higgs search for Higgs masses close to $2M_{\rm W}$. It is the first channel at the LHC to set exclusion limits in some Higgs mass ranges, and is a very promising discovery channel. As Figure 2 shows, the Higgs branching ratio into WW is close to unity at

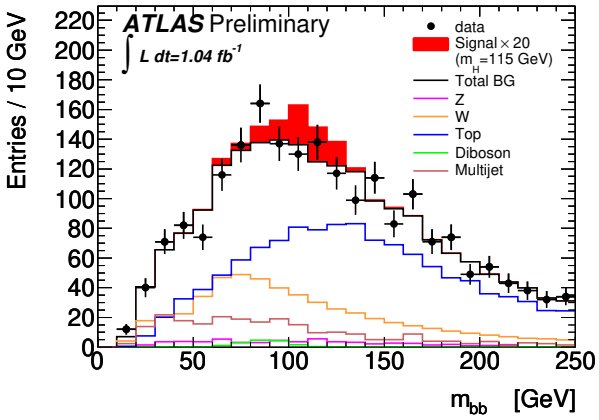


Figure 5: $m_{\mathrm{b\bar{b}}}$ distribution in data, for a 115 GeV Higgs signal and for the various backgrounds. The MC prediction for signal has been amplified by a factor of 20 for visibility.

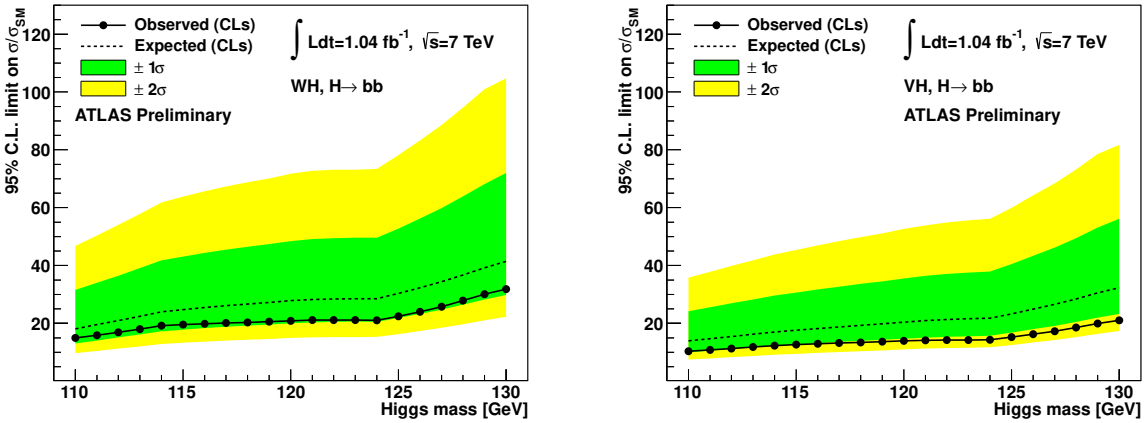


Figure 6: Expected (dashed) and observed (solid line) exclusion limits from the $WH \to l\nu bb$ channel alone *(left)* and from the $WH \to l\nu bb$ and $ZH \to llbb$ channels combined *(right)*.

$2M_{\mathrm{W}}$, and remains large for higher masses up to a TeV. For reference, the cross-section $\times$ branching ratio of the process $H \to WW^{(*)} \to l\nu l\nu$ is about 0.36 pb for $M_{\mathrm{H}} = 150$ GeV.

The analysis presented here covers the range of $110 < m_{\mathrm{H}} < 240$ GeV. The analysis is divided into six final states based on the leptonic decay modes of the W pair and the jet multiplicity: ee, $e\mu$, $\mu\mu$, each accompanied by either no jet or exactly 1 jet. The event selection basically involves selecting two high-p_{T} isolated leptons and large $E_{\mathrm{T}}^{\mathrm{miss}}$.

3.1. Event selection

As in the WH analysis, lowest-threshold unprescaled triggers are used. In this case, the trigger requirement depends on the final state:

- ee: single electron trigger with 20 GeV threshold
- $\mu\mu$: OR of two single muon triggers, with thresholds at 18 GeV and 40 GeV[1]

[1]The 40 GeV threshold trigger is used to increase acceptance in the barrel region of the detector.

- $e\mu$: OR of the above three triggers

The intial event selection, termed *pre-selection*, is described below:

- Exactly two leptons in the event, the higher-p_{T} ('leading') lepton having $p_{\mathrm{T}} > 25$ GeV. The lower-p_{T} ('sub-leading') lepton must have $p_{\mathrm{T}} > 20$ GeV for electrons and $p_{\mathrm{T}} > 15$ GeV for muons.
- In the ee and $\mu\mu$ channels, the dilepton invariant mass $m_{\mathrm{ll}} > 15$ GeV to reject a low mass Drell-Yan background. In addition, $|m_{\mathrm{ll}} - m_{\mathrm{Z}}| > 15$ GeV to reject Z background. Finally, the relative missing transverse energy, $E_{\mathrm{T,rel}}^{\mathrm{miss}} > 40$ GeV. $E_{\mathrm{T,rel}}^{\mathrm{miss}}$ is defined as:

$$E_{\mathrm{T,rel}}^{\mathrm{miss}} = \begin{cases} E_{\mathrm{T}}^{\mathrm{miss}} & \text{if } \Delta\phi \geq \pi/2 \\ E_{\mathrm{T}}^{\mathrm{miss}} \cdot \sin\Delta\phi & \text{if } \Delta\phi < \pi/2 \end{cases}, \tag{1}$$

  where $\Delta\phi$ is the absolute value of the difference in the azimuthal angle ϕ between the $E_{\mathrm{T}}^{\mathrm{miss}}$ and the nearest lepton with $p_{\mathrm{T}} > 15$ GeV or jet with $p_{\mathrm{T}} > 25$ GeV.
- In the $e\mu$ channel, $m_{\mathrm{ll}} > 10$ GeV and $E_{\mathrm{T,rel}}^{\mathrm{miss}} > 25$ GeV.

Following the pre-selection, the events are divided into 0-jet and 1-jet bins. For this purpose, each jet is required to have $p_{\mathrm{T}} > 25$ GeV and $|\eta| < 4.5$. Figure 7 shows the jet multiplicity distribution after the $E_{\mathrm{T,rel}}^{\mathrm{miss}}$ cut for data, for MC signal and for various background predictions.

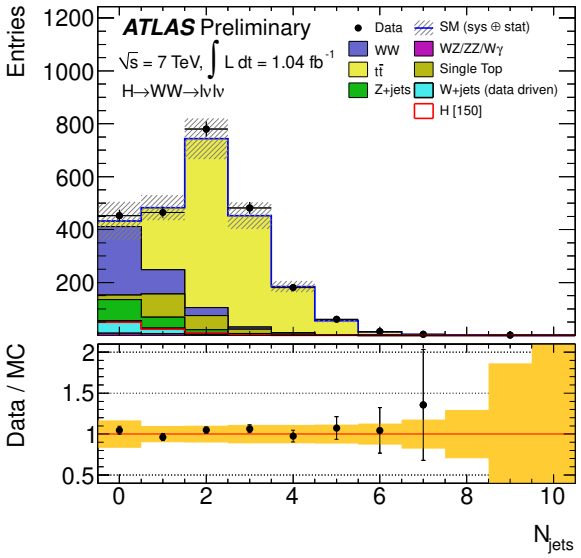


Figure 7: Jet multiplicity after the cut on $E_{\mathrm{T,rel}}^{\mathrm{miss}}$. The bin-by-bin ratio between data and the background expectation is also shown, with the overall systematic uncertainty in the normalizations indicated by the yellow band.

At this stage, different cuts are applied to events depending on the jet bin. In the 0-jet bin, the transverse momentum of the dilepton system, $p_{\mathrm{T}}^{\mathrm{ll}}$, must be greater than 30 GeV. Then a series of topological cuts is applied depending on the Higgs mass:

- $m_{\mathrm{H}} < 170$ GeV: $m_{\mathrm{ll}} < 50$ GeV; the dilepton opening angle, $\Delta\phi_{\mathrm{ll}} < 1.3$.
- $m_{\mathrm{H}} >= 170$ GeV: $m_{\mathrm{ll}} < 65$ GeV; $\Delta\phi < 1.8$.
- The transverse mass m_{T} must satisfy $0.75 \times m_{\mathrm{H}} < m_{\mathrm{T}} < m_{\mathrm{H}}$, where

$$m_{\mathrm{T}} = \sqrt{(E_{\mathrm{T}}^{\ell\ell} + E_{T}^{\mathrm{miss}})^2 - (\mathbf{P}_{\mathrm{T}}^{\ell\ell} + \mathbf{P}_{\mathrm{T}}^{\mathrm{miss}})^2}, \tag{2}$$

with $E_{\mathrm{T}}^{\ell\ell} = \sqrt{(\mathbf{P}_{\mathrm{T}}^{\ell\ell})^2 + m_{\ell\ell}^2}$, $|\mathbf{P}_{\mathrm{T}}^{\mathrm{miss}}| = E_{T}^{\mathrm{miss}}$ and $\mathbf{P}_{\mathrm{T}}^{\ell\ell}$ is the transverse momentum of the dilepton system.

	Signal	WW	W+jets	Z/γ^*+jets	$t\bar{t}$	$tW/tb/tqb$	$WZ/ZZ/W\gamma$	Total Bkg.	Observed
$ee+e\mu+\mu\mu$	0.73 ± 0.16	111 ± 15	13 ± 7	2 ± 3	10 ± 4	8 ± 2	4.3 ± 1.2	150 ± 30	153
ee	0.01 ± 0.07	13 ± 2	2 ± 2	0.2 ± 1.7	1.4 ± 1.6	0.5 ± 1.0	0 ± 2	17 ± 5	28
$e\mu$	0.73 ± 0.17	76 ± 10	9 ± 6	< 0.01	6 ± 3	4.6 ± 1.4	3 ± 2	100 ± 20	98
$\mu\mu$	< 0.14	23 ± 3	1.8 ± 1.2	1.9 ± 1.2	2.2 ± 1.7	2.6 ± 1.1	1 ± 2	32 ± 6	27

Table III: Expected and observed event numbers after all cuts in the WW control region for the 0-jet channel in 1.04 fb^{-1} of data. The signal numbers correspond to $m_{\rm H} = 150$ GeV.

In the 1-jet channel, a b-jet veto is applied to reduce top background. The magnitude of the total $p_{\rm T}$ of the Higgs boson and jet system, defined as $\mathbf{P}_{\rm T}^{\rm tot} = \mathbf{P}_{\rm T}^{\rm l1} + \mathbf{P}_{\rm T}^{\rm l2} + \mathbf{P}_{\rm T}^{\rm j} + \mathbf{P}_{\rm T}^{\rm miss}$, is required to be less than 30 GeV. Finally, the same topological selection as in the 0-jet case is applied.

3.2. Background processes

WW: Continuum WW production is the largest background in the 0-jet channel. A dedicated control region in data is used to derive the WW normalization in the signal region. This control region is defined using the same pre-selection as for the signal region, but requiring $m_{\rm ll} > 80$ GeV and removing the topological cuts. Table III shows the expected number of signal and background events in the WW control region, together with the observed number of events in data.

Top: $t\bar{t}$ and single top constitute the largest background in the 1-jet channel. The signal region normalization for these backgrounds is determined from a control region in data defined by reversing the b-jet veto and removing the topological cuts.

W+jets: This background is estimated using a fully data-driven method. A control sample in data is obtained by requiring one lepton in the events to pass the full set of selection criteria listed in Section 3.1, while the other lepton must pass a looser set of criteria. A normalization *fake factor* is extracted from a dijet data sample, which is then applied to the control sample to estimate the $W + jets$ contamination in the signal region.

Z+jets: The *Z+jets* background prediction is taken from MC, normalized by a $E_{\rm T}^{\rm miss}$ mismodelling factor obtained from a data/MC comparison in two control regions.

WZ, ZZ, Wγ: These backgrounds are small, and are estimated from MC.

3.3. Results: 0-jet channel

Table IV shows the expected number of signal and background events, as well as the observed events in data, after applying each 0-jet selection. We observe a small excess in data in the $\mu\mu$ channel after all cuts. Figure 8 shows the $\Delta\phi_{\rm ll}$ and the $m_{\rm T}$ distributions in data and for signal and background expectations. The data seems to be systematically higher than the expectation.

Selection	Signal	WW	W+jets	Z/γ^*+jets	$t\bar{t}$	$tW/tb/tqb$	$WZ/ZZ/W\gamma$	Total Bkg.	Observed
Jet Veto	50 ± 11	260 ± 30	46 ± 17	80 ± 70	22 ± 8	17 ± 4	7.8 ± 1.5	430 ± 100	453
$\lvert\mathbf{P}_{\rm T}^{\ell\ell}\rvert > 30$ GeV	48 ± 10	230 ± 20	38 ± 14	15 ± 6	19 ± 7	16 ± 4	7.3 ± 1.4	330 ± 50	371
$m_{\ell\ell} < 50$ GeV	34 ± 7	59 ± 8	11 ± 3	7 ± 4	2.7 ± 1.8	2.8 ± 0.8	0.9 ± 0.3	83 ± 11	116
$\Delta\Phi_{\ell\ell} < 1.3$	30 ± 7	46 ± 6	5.8 ± 1.8	5 ± 3	2.7 ± 1.7	2.8 ± 0.8	0.8 ± 0.2	63 ± 9	89
$0.75 \times m_H < m_{\rm T} < m_H$	21 ± 4	26 ± 3	2.9 ± 0.9	1 ± 2	1.6 ± 1.2	0.7 ± 0.4	0.6 ± 0.2	33 ± 5	49
ee	3.1 ± 0.7	3.7 ± 0.7	0.5 ± 0.2	0.4 ± 0.6	0.0 ± 0.6	0.0 ± 0.2	0.05 ± 0.19	4.7 ± 1.2	7
$e\mu$	11 ± 2	13.4 ± 1.9	1.7 ± 0.7	< 0.01	1.1 ± 0.8	0.4 ± 0.3	0.4 ± 0.3	17 ± 2	21
$\mu\mu$	6.9 ± 1.5	8.8 ± 1.3	0.7 ± 0.5	0.5 ± 2.0	0.4 ± 0.8	0.3 ± 0.3	0.18 ± 0.19	11 ± 3	21

Table IV: Expected and observed event numbers after applying each cut for the 0-jet channel in 1.04 fb^{-1} of data. The signal numbers correspond to $m_{\rm H} = 150$ GeV. The W+jets background expectation is purely data-driven. The uncertainties shown include both statistical and systematic components.

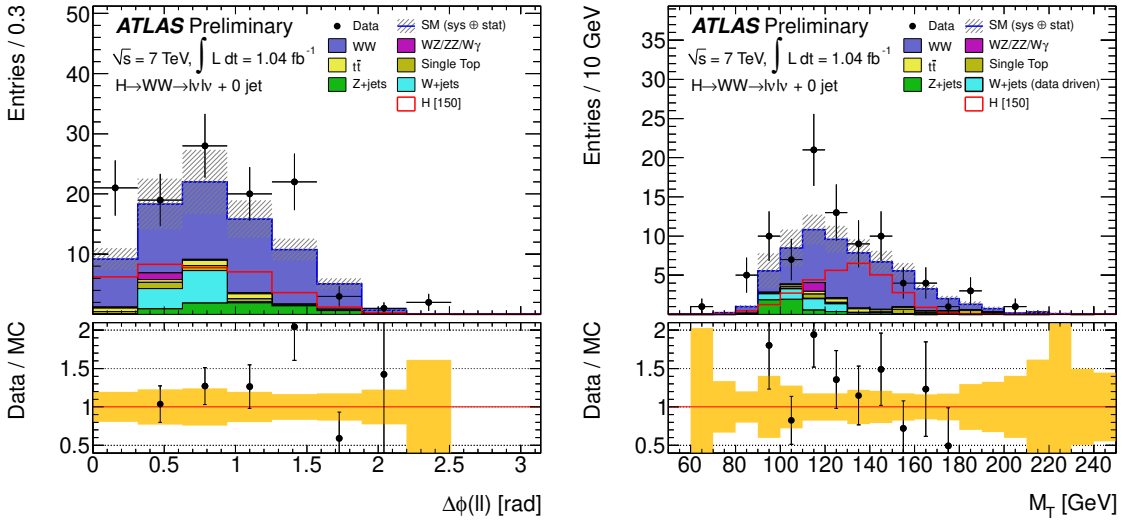


Figure 8: Distributions of the dilepton opening angle $\Delta\phi_{ll}$ *(left)* and of the transverse mass m_T *(right)* in the 0-jet channel after the cut on m_{ll}. The bin-by-bin ratio between data and the background expectation is also shown, with the overall systematic uncertainty indicated by the yellow band.

3.4. Results: 1-jet channel

Table V shows the expected number of signal and background events and the observed events in data after applying each 1-jet selection. As in the 0-jet case, we see a small excess in data in the $\mu\mu$ channel after all cuts. Figure 9 shows the $\Delta\phi_{ll}$ and the m_T distributions in data and for signal and background expectations. The same trend is seen in the data-MC comparison as in the 0-jet case.

Selection	Signal	WW	W+jets	Z/γ^*+jets	$t\bar{t}$	$tW/tb/tqb$	$WZ/ZZ/W\gamma$	Total Bkg.	Observed
1 jet	23 ± 4	92 ± 9	20 ± 10	40 ± 30	240 ± 60	88 ± 13	6.2 ± 0.8	490 ± 70	465
b-jet veto	23 ± 4	91 ± 9	19 ± 10	40 ± 30	140 ± 40	45 ± 7	6.1 ± 0.8	340 ± 50	333
$\lvert\mathbf{P}_T^{\rm tot}\rvert < 30$ GeV	19 ± 3	76 ± 8	9 ± 5	25 ± 19	80 ± 20	35 ± 6	4.1 ± 0.5	230 ± 40	221
$Z \to \tau\tau$ veto	19 ± 4	74 ± 8	9 ± 5	20 ± 10	80 ± 19	33 ± 5	4.0 ± 0.7	220 ± 17	212
$m_{\ell\ell} < 50$ GeV	13 ± 3	16 ± 3	1.2 ± 0.5	3.4 ± 1.6	12 ± 4	7.2 ± 1.7	0.9 ± 0.2	41 ± 5	56
$\Delta\Phi_{\ell\ell} < 1.3$	11 ± 2	13 ± 2	1.0 ± 0.5	1.5 ± 1.2	11 ± 4	6.3 ± 1.5	0.74 ± 0.20	33 ± 5	44
$0.75 \times m_H < m_T < m_H$	7.2 ± 1.6	6.2 ± 1.3	0.5 ± 0.9	0.4 ± 0.6	4.9 ± 1.7	2.3 ± 0.7	0.34 ± 0.16	15 ± 3	21
ee	0.9 ± 0.3	0.8 ± 0.3	0.08 ± 0.04	0.0 ± 0.4	0.8 ± 1.0	0.2 ± 0.4	0.06 ± 0.08	2.0 ± 1.2	4
$e\mu$	4.0 ± 0.9	3.5 ± 0.8	0.4 ± 0.2	0.4 ± 0.7	3.1 ± 1.3	1.2 ± 0.6	0.24 ± 0.13	8.8 ± 1.9	8
$\mu\mu$	2.3 ± 0.5	1.9 ± 0.4	0.0 ± 0.8	0.0 ± 0.4	1.1 ± 1.1	0.8 ± 0.7	0.04 ± 0.07	3.9 ± 1.7	9

Table V: Expected and observed event numbers after applying each cut for the 1-jet channel in 1.04 fb^{-1} of data. The signal numbers correspond to $m_H = 150$ GeV. The W+jets background expectation is purely data-driven. The uncertainties shown include both statistical and systematic components.

3.5. Exclusion limits

Figure 10 *(left)* shows the exclusion limit on the standardized cross-section $\mu = \sigma/\sigma_{\rm SM}$ from the $H \to WW^{(*)} \to l\nu l\nu$ channel. The Standard Model Higgs is excluded in the mass range of $158 < m_H < 186$ GeV at the 95% confidence level, the expected limit being $142 < m_H < 186$ GeV. Figure 10 *(right)* shows the signal significances as functions of the Higgs mass. In the range $126 < m_H < 158$ GeV, an excess in data corresponding to larger than 2σ significance is observed. The largest excess is observed at $m_H \approx 130$ GeV, and corresponds to about 2.7σ.

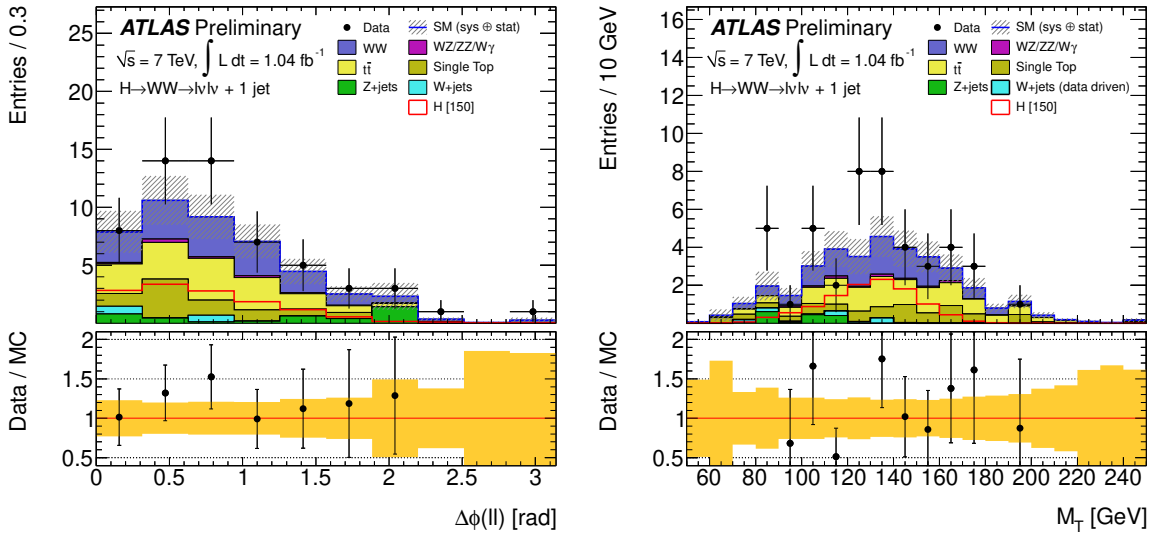


Figure 9: *Left*: Distributions of the dilepton opening angle $\Delta\phi_{\ell\ell}$ and of the transverse mass m_{T} *(right)* in the 1-jet channel after the cut on $m_{\ell\ell}$. The bin-by-bin ratio between data and the background expectation is also shown, with the overall systematic uncertainty indicated by the yellow band.

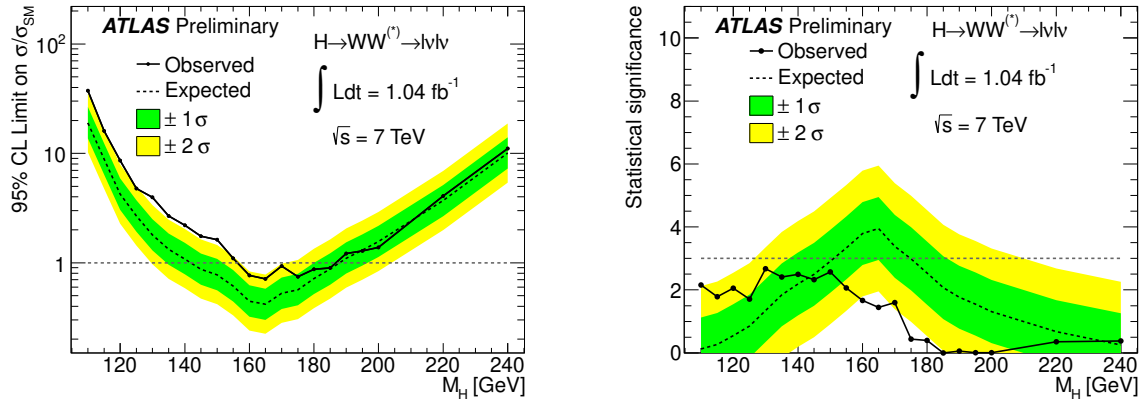


Figure 10: *Left*: Expected (dashed) and observed (solid line) exclusion limits from the $H \to WW^{(*)} \to l\nu l\nu$ channel; *right*: the expected (dashed) and observed (solid) signal significances for a SM Higgs boson production vs m_{H}.

4. Conclusion

We have presented results of the SM Higgs search by ATLAS in the $WH \to l\nu bb$ and $H \to WW^{(*)} \to l\nu l\nu$ channels using 1.04 fb^{-1} of data collected in 2011. The $WH \to l\nu bb$ channel sets limits on the Higgs production cross-section that are 15-30 times the Standard Model cross-section in the range $110 < m_{\mathrm{H}} < 130$ GeV, while the $H \to WW^{(*)} \to l\nu l\nu$ channel excludes the SM Higgs in the range of $158 < m_{\mathrm{H}} < 186$ GeV at the 95% confidence level.

Expected improvements to both analyses are going to include multivariate approaches, reduced systematics uncertainties and a boosted Higgs analysis in the $H \to b\bar{b}$ channel.

References

1 "Search for the Standard Model Higgs boson produced in association with a vector boson and decaying to a b-quark pair with the ATLAS detector at the LHC", ATLAS-CONF-2011-103, CERN, Geneva, July 2011.